HHS Public Access

Author manuscript

Neurobiol Dis. Author manuscript; available in PMC 2022 January 01.

Published in final edited form as:

Neurobiol Dis. 2021 January ; 147: 105148. doi:10.1016/j.nbd.2020.105148.

Distinct Poly(A) nucleases have differential impact on *sut-2* dependent tauopathy phenotypes.

Rebecca L. Kow[a,b], **Timothy J. Strovas**[a], **Pamela J. McMillan**[b,c], **Ashley M. Jacobi**[d], **Mark A. Behlke**[d], **Aleen D. Saxton**[a], **Caitlin S. Latimer**[e], **C. Dirk Keene**[e], **Brian C. Kraemer**[a,b,c,e,*]

[a]Geriatrics Research Education and Clinical Center, Veterans Affairs Puget Sound Health, Care System, Seattle, WA 98108, USA

[b]Division of Gerontology and Geriatric Medicine, Department of Medicine, University of Washington, Seattle, WA 98104, USA

[c]Department of Psychiatry and Behavioral Sciences, University of Washington, Seattle, WA 98195, USA

[d]Integrated DNA Technologies, Coralville, IA 52241, USA

[e]Department of Pathology, University of Washington, Seattle, WA 98195, USA

Abstract

Aging drives pathological accumulation of proteins such as tau, causing neurodegenerative dementia disorders like Alzheimer's disease. Previously we showed loss of function mutations in the gene encoding the poly(A) RNA binding protein SUT-2/MSUT2 suppress tau-mediated neurotoxicity in *C. elegans* neurons, cultured human cells, and mouse brain, while loss of PABPN1 had the opposite effect (Wheeler et al., 2019). Here we found that blocking poly(A) tail extension with cordycepin exacerbates tauopathy in cultured human cells, which is rescued by MSUT2 knockdown. To further investigate the molecular mechanisms of poly(A) RNA-mediated tauopathy suppression, we examined whether genes encoding poly(A) nucleases also modulated tauopathy in a *C. elegans* tauopathy model. We found that loss of function mutations in *C. elegans ccr-4* and *panl-2* genes enhanced tauopathy phenotypes in tau transgenic *C. elegans* while loss of *parn-2* partially suppressed tauopathy. In addition, loss of *parn-1* blocked tauopathy suppression by loss of *parn-2*. Epistasis analysis showed that *sut-2* loss of function suppressed the tauopathy enhancement caused by loss of *ccr-4* and SUT-2 overexpression exacerbated tauopathy even in the

*Corresponding author at: Seattle Veterans Affairs Puget Sound Health Care System, S182, 1660 South Columbian Way, Seattle, WA 98108, USA. kraemerb@u.washington.edu (B.C. Kraemer).

Author contributions

BK and RK conceptualized the study; RK, TS, PM performed the experiments. RK, TS, PM, BK performed data analysis. RK, TS, AS, CDK, CL, AJ, MB, BK provided essential experimental resources. RK, TS, PM, AS provided graphical representations of data. RK and BK wrote the original draft; all authors made essential intellectual contributions to multiple revised drafts.

Declaration of Competing Interest

AJ and MB are employed by Integrated DNA Technologies, Inc., (IDT) which offers reagents for sale similar to some of the compounds described in the manuscript. AJ and MB own equity in DHR, the parent company of IDT. All other authors declare no conflicts of interest.

Appendix A. Supplementary data

Supplementary data to this article can be found online at https://doi.org/10.1016/j.nbd.2020.105148.

presence of *parn-2* loss of function in tau transgenic *C. elegans*. Thus *sut-2* modulation of tauopathy is epistatic to *ccr-4* and *parn-2*. We found that human deadenylases do not colocalize with human MSUT2 in nuclear speckles; however, expression levels of TOE1, the homolog of *parn-2*, correlated with that of MSUT2 in post-mortem Alzheimer's disease patient brains. Alzheimer's disease patients with low TOE1 levels exhibited significantly increased pathological tau deposition and loss of NeuN staining. Taken together, this work suggests suppressing tauopathy cannot be accomplished by simply extending poly(A) tails, but rather a more complex relationship exists between tau, *sut-2/MSUT2* function, and control of poly(A) RNA metabolism, and that *parn-2/TOE1* may be altered in tauopathy in a similar way.

Keywords

Tau; SUTSUT-2; MSUT2; Poly(A) deadenylases; TOE1; Neurofibrillary tangles; PARN; CCR4; Neurodegeneration

1. Introduction

Abnormal intracellular inclusions composed of the microtubule-binding protein tau are seen in a number of age-associated neurodegenerative diseases called tauopathies (Irwin, 2016). The most prevalent tauopathy, Alzheimer's disease (AD), is the most common cause of dementia (Gaugler et al., 2016) and it is the burden (extent) of tau tangles, rather than the burden (density or distribution) of amyloid plaques, that most strongly correlates with cognitive decline in AD (Bierer et al., 1995; Riley et al., 2002; Tiraboschi et al., 2004). Additionally, multiple mutations in the *MAPT* gene, which encodes tau protein, have been directly linked or associated with frontotemporal dementia with parkinsonism-17 (Irwin, 2016; Wang and Mandelkow, 2016). Not only are there still no pharmacological treatments that reverse or cure tauopathies, the molecular disease mechanisms underlying tauopathy are still unclear (Khanna et al., 2016; Wang and Mandelkow, 2016).

To further understand mechanisms of tauopathy and to discover novel genes and pathways that regulate tauopathy, we previously developed a *C. elegans* model that expresses human tau in all its neurons (Kraemer et al., 2003). Phenotypes seen with this model include uncoordinated locomotion, accumulation of insoluble tau, neuron loss, and shortened life span (Kraemer et al., 2003). We have used this model to screen for novel modifiers of tauopathy including forward mutagenesis screens (Guthrie et al., 2009; Kraemer and Schellenberg, 2007), whole genome RNAi screening (Kraemer et al., 2006), and chemical drug library screening (McCormick et al., 2013).

sut-2 was identified as a novel suppressor of tauopathy in forward mutagenesis screening of tau transgenic *C. elegans* (Guthrie et al., 2009). Loss of function mutations reversed locomotor deficits, decreased insoluble tau accumulation, and reduced neurodegeneration. The mammalian homolog, MSUT2, was also shown to modulate tauopathy in mouse models of tauopathy (Wheeler et al., 2019). Additionally, MSUT2 protein levels are altered in Alzheimer's disease and associated with changes in tau pathology, inflammation, and age of disease onset (Wheeler et al., 2019).

Not much is known about the molecular function of MSUT2; MSUT2 has been shown to bind to poly(A) RNA and to the protein PABPN1, and together MSUT2 and PABPN1 localize to nuclear speckles (Wheeler et al., 2019). MSUT2 and PABPN1 have opposing effects on poly(A) tail length of mRNAs and tauopathy. MSUT2 knockdown by siRNA increases overall poly(A) tail lengths of mRNAs while PABPN1 knockdown decreases poly(A) tail length (Kelly et al., 2014). MSUT2 knockdown reduces insoluble and phosphorylated tau in a human cell culture model of tauopathy while PABPN1 knockdown increases insoluble and phosphorylated tau (Wheeler et al., 2019).

Poly(A) polymerases and poly(A) deadenylases also regulate poly(A) tail length of mRNAs (Eckmann et al., 2011; Zhang et al., 2010). Poly(A) polymerase activity increases poly(A) tail length while poly(A) deadenylase activity reduces poly(A) tail length. Controlling poly(A) tail length is important for mRNA stability and translation; while classically long poly(A) tails are thought to stabilize mRNA and stimulate translation of mRNA (Eckmann et al., 2011), a recent study has shown that shorter poly(A) tails are more common among highly-expressed genes in somatic cells and suggests that appropriate pruning of poly(A) tails is important for efficient translation (Lima et al., 2017). Since loss of MSUT2 leads to lengthened poly(A) tails, loss of poly(A) deadenylase expression could lead to the equivalent effect on poly(A) tails as well as on tauopathy. Various poly(A) deadenylases such as CCR4-NOT, PAN2/PAN3, and PARN are conserved from yeast to *C. elegans* to mammals and have distinct cellular localizations, regulatory mechanisms, and functions (Yan, 2014). Two genes that encode poly(A) deadenylases have been previously shown to modulate tauopathy in the *C. elegans* tauopathy model (Kraemer et al., 2006; Wheeler et al., 2019). Interestingly, loss of these genes enhanced tauopathy. To better understand how these various poly(A) deadenylases might modulate tauopathy, we screened a collection of poly(A) deadenylase gene mutants against the *C. elegans* tauopathy model. We found that some deadenylases could modulate tauopathy but did so differently than *sut-2*.

2. Materials and methods

2.1. Cell culture, cordycepin treatment, and RNA interference

HEK293 and HEK/tau cells (100 μg/mLL Zeocin) were cultured under standard tissue culture conditions (DMEM, 10% defined fetal bovine serum, Penicillin (1000 IU/mL) Streptomycin (1000 μg/mL) as previously described (Wheeler et al., 2019). Small interfering RNAs (siRNAs) were obtained from Integrated DNA Technologies (Coralville, IA). RNA interference and plasmid transient transfections were conducted following manufacture's protocol (RNAiMAX, Invitrogen). Cells were fixed 96 h after transfection. For cordycepin treatment, cells were dosed with 100 mg/mL cordycepin (Tocris, catalog# 2294) 2 h prior to fixation.

2.2. C. elegans strains, genome editing, and transgenics

N2 (Bristol) was used as wild type *C. elegans* (Brenner, 1974). *C. elegans* alleles used in this study are listed in Table 1. *bk3002, bk3045,* and *bk3046* were generated using CRISPR. All other strains containing desired alleles were obtained from the National Bioresource Project (Japan) or the *C. elegans* Genetics Center (CGC). *C. elegans* mutants were crossed into the

tau transgenic *C. elegans* strain CK10 (*bkIs10[aex-3p::tau-V337M], myo-2p::GFP*) expressing human 4R1N tau with a V337M mutation (Kraemer et al., 2003). The presence of alleles of interest was verified with PCR genotyping. All strains were maintained at 20 °C on standard NGM plates containing OP50 *Escherichia coli* as previously described (Brenner, 1974). For protein studies, worms were grown on NGM plates containing 5× more peptone (5XPEP) prior to collection.

Two independent null *sut-2 alleles (bk3001, bk3002)* and two independent *parn-2* alleles *(bk3045, bk3046)* were generated using CRISPR-Cas9 genome editing technology by introducing purified active recombinant Cas9 protein and synthetic CRISPR guide RNAs (gRNAs) as previously described (Paix et al., 2015).

S.p. crRNA name	Protospacer	Relative Position in gene
parn-2 null 5′	AAAAATCGATAAAATTAGGG	parn2 start codon
parn-2 null 3′	TAACAATCAAGATCAGGTGG	parn2 stop codon
sut-2 null 5′	AGAGACTAGTAAAAAGGAGG	sut-2 promoter
sut-2 null 3′	GGACTAGTTAGCTGTGGCGG	sut-2 stop codon

Cas9 gRNAs were prepared by mixing equimolar amounts (0.5 μg/uL) of Alt-R crRNA and Alt-R tracrRNA (Integrated DNA Technologies) and then the gRNAs were complexed to equimolar quantities of Cas9 protein (Alt-R S.p. Cas9 Nuclease V3, Integrated DNA Technologies as described). *dpy-10* was utilized as a gene co-conversion marker as previously described (Arribere et al., 2014) and removed by outcrossing. For each genome editing effort, two gRNAs were introduced targeting the promoter/start codon and 3'UTR/stop codon sequences of the *sut-2* and *parn-2* genomic loci respectively to generate null alleles.

2.3. Behavior in C. elegans

NGM plates containing 4-day-old tau transgenic *C. elegans* or 3-day-old non-transgenic *C. elegans*, corresponding to roughly day 1 adult *C. elegans*, were flooded with 1 mL of M9 buffer. Swimming worms were pipetted onto a 35 mm unseeded NGM plate. 1 min following the addition of M9 buffer videos of swimming worms were recorded for 1 min at 14 frames per second. Videos were analyzed using WormLab 2019 (MBF Bioscience). The frequency of body bends, defined as "turns" by the software, was quantified. A turn was defined as a change in the body angle defined by the quarter points and midpoint of the worm that was at least 20 degrees positive or negative from a straight line. Worms that were tracked for less than 20 s were omitted from analysis. At least 50 worms were counted per strain when comparing non-transgenic *C. elegans* to deadenylase mutants and at least 100 worms from at least 3 independent samples were counted per strain when comparing tau transgenic *C. elegans* to tau transgenic *C. elegans* containing deadenylase mutations.

2.4. Poly(A) tail length assay

Staged young adult tau transgenic *C. elegans* were grown from eggs at 20 °C for 3 days on 5XPEP plates, washed off plates in M9 buffer, and collected by centrifugation. RNA was

extracted from ~100 μL of packed worms per sample using Tri-Reagent (Molecular Research Center) as per manufacturer instructions. Poly(A) tail lengths were assayed using the USB Poly(A) Tail-Length Assay Kit (Affymetrix) as per manufacturer instructions with the following modification to the PCR amplification step. The PCR reaction consisted of 10 μL of HotStart Taq, 7 μL of nuclease-free water, 0.5 μL of 10 μM gene-specific primer (see below), 0.5 μL of 10 μM Universal PCR Reverse Primer, and 2 μL of the diluted reverse transcription sample. A three-step PCR reaction with 40 cycles of amplification was used to amplify the signal. PCR products were run on a QIAexcel Advanced capillary electrophoresis instrument (Qiagen) using a QIAxcel DNA high resolution Kit with QX DNA Size Marker pUC18/*Hae*III (catalog #929550) at 20 ng/uL and QX alignment marker 15 bp/600 bp (catalog #929530). Samples were processed using the 0M400 method with a 20 s sample injection time and analyzed with the QIAxcel ScreenGel Software for major peak, median signal, and concentration.

Gene of interest	Primer sequence	Distance from end of 3′ UTR
act-1	ACCACCAGCTTTCTATTTCTTGTTTGC	149
snb-1	TGATCCCACATCCACATGAGCTTATC	132
unc-54	AAAAATTGTGCTCCCTCCCC	103

2.5. Tau extraction and immunoblotting

Staged young adult tau transgenic *C. elegans* were grown from eggs at 20 °C for 3 days on 5XPEP plates, washed off plates in M9 buffer, and collected by centrifugation. Worms were snap frozen in liquid nitrogen and stored at −70 °C. tau fractions were obtained as described previously (Kow et al., 2018) with some modifications. 2 μL of RAB Hi-Salt buffer (0.1 M MES, 1 mM EGTA, 0.5 mM $MgSO_4$, 0.75 M NaCl, 0.02 M NaF, pH 7.0) containing PMSF and protease inhibitors was added per mg of worm pellet and homogenized by sonication. A portion of the sample was saved for immunoblotting (for total tau and tubulin) while the rest was centrifuged at 40,000 xg, 4 °C for 40 min. The supernatant was saved as the RAB/soluble fraction. The pellet was extracted by adding 1 μL of RIPA buffer (50 mM Tris, 150 mM NaCl, 1% Nonidet P-40, 5 mM EDTA, 0.5% deoxycholate, 0.1% SDS, pH 8.0) containing PMSF and protease inhibitors per mg of original worm pellet weight and centrifuged at 40,000 xg, 4 °C for 20 min. The supernatant was saved as the RIPA/detergent soluble fraction. The pellet was extracted again by adding 2 μL 70% formic acid (FA) per mg of original worm pellet weight and centrifuged at 13,000 xg, 4 °C for 15 min. The supernatant was the FA/detergent insoluble fraction. This fraction was dried in a speed vacuum concentrator until only a dry film remained in the tube.

Protein samples were diluted with 5× sample buffer (0.046 M Tris, 0.005 M EDTA, 0.2 M dithiothreitol, 50% sucrose, 5% sodium dodecyl sulfate, 0.05% bromophenol blue), boiled for 5 min., and centrifuged at 13,000 xg for 2 min. Prior to being loaded onto 4–15% pre-cast Criterion sodium dodecyl sulfate polyacrylamide gel electrophoresis gradient gels and transferred to PVDF membranes as recommended by the manufacturer (Bio-Rad). Total protein samples were diluted 2-fold with 5× sample buffer. FA/insoluble fractions were

resuspended with 2× sample buffer at 2 μL per mg of original worm pellet weight. All other protein samples were diluted 5-fold with 5× sample buffer. 5–20 μL of diluted sample was loaded for each analysis. Primary antibodies used were rabbit monoclonal anti-tau antibody (Rockland) at 1:5000 and mouse anti-tubulin antibody E7 (Developmental Studies Hybridoma Bank) at 1:5000. Secondary antibodies used were anti-rabbit HRP (Jackson Immuno Research) and anti-mouse HRP (Jackson Immuno Research) at 1:5000. ECL substrate (Bio-Rad) was added to the membrane and chemiluminescence signals were detected with ChemiDoc-It Imager (UVP) and measured with UVP Software.

2.6. Immunohistochemistry

Immunohistochemistry for TOE1 was performed on 5-μm paraffin-embedded frontal cortex sections from 15 AD cases and 16 normal control cases. Brain sections were deparaffinized, rehydrated through ethanols and microwaved in citrate buffer for antigen retrieval. Sections were treated for endogenous peroxidases, blocked in 5% milk, incubated with anti-TOE1 polyclonal antibody (Invitrogen, PA5-30948) overnight at 4 °C, followed by biotinylated rabbit secondary antibody. Sections were incubated with an avidin-biotin complex (Vector, Vectastain Elite ABC kit) and the reaction product was visualized with 0.05% diaminobenzidine (DAB)/0.01% hydrogen peroxide. Our AD cohort was previously characterized as being MSUT2 positive or MSUT2 depleted and pTau burden (AT180) and neuronal loss (reduced NeuN immunoreactivity) was correlated with loss of MSUT2 (Wheeler et al., 2019). In the current study, the AD cohort was re-classified based on TOE1 immunostaining as AD, TOE1 positive and AD, TOE1 depleted, and it was determined that TOE1 expression corresponded with MSUT2 expression. *Re*-analysis of the quantitation of AT180 and NeuN immunoreactivity based on this TOE1 classification was performed to determine if pTau burden and neuronal loss also correlated with TOE1 depletion. Data were averaged and are represented as means +/− SEM. A two-tailed Student's *t*-test was used to assess differences in staining intensity between the TOE1 positive and TOE1 depleted groups.

2.7. Fluorescent immunohistochemistry

Cells were grown on poly-D-lysine coated 12 mm round coverslips and fixed in 4% formaldehyde solution. Cells were washed 3 × 5 min in PBS/Ca^{2+}/Mg^{2+}, then blocked in antibody buffer (PBS, 0.5% Triton X-100, 1 mM EDTA, 0.1% BSA, 0.05% NaN_3) with 10% normal goat serum. Primary antibodies were applied and incubated for 1 h at room temperature. Primary antibodies used were: pTau = AT180 (Thermo Fisher), TOE1 = Thermo Fisher (Catalog# PA5-30948), PARN = Protein Tech (Catalog# 13799-1AP), PAN2 = Protein Tech (Catalog# 16427-1AP), CNOT6 = Cell Signal (Catalog# 13415). Cells were washed 3 × 5 min in PBS/Ca^{2+}/Mg^{2+}, then re-blocked for 10 min. Appropriate Alexa dye-labeled secondary antibodies (Invitrogen) were applied and incubated for 20 min at room temperature. Cells were again washed 3 × 5 min in PBS/Ca^{2+}/Mg^{2+}, counterstained with 300 nM DAPI and mounted with ProLong Gold antifade (Molecular Probes). Microscopy was performed on a Delta Vision microscope (GE, Inc) using a 100× oil immersion objective, a sCMOS camera, and 2 × 2 binning. Image analysis was performed using softWoRx 6.0 Beta software (GE, Inc).

2.8. Human tissue

We obtained samples of postmortem tissue from the University of Washington Alzheimer's Disease Research Center (ADRC) Neuropathology Core (PI, Dr. C. Dirk Keene) after receiving human subjects' approval (University of Washington Human Subjects Division approval: HSD# 06-0492-E/A 01). We selected AD cases on the basis of having autopsy-confirmed AD (Braak stages V or VI with CERAD score of moderate or frequent). Control samples came from age matched neurologically healthy control participants with low levels of AD pathology (Braak stage III or less and CERAD scores of none or sparse).

3. Results

3.1. General inhibition of Poly(A) addition provokes pathological tau accumulation in an MSUT2 dependent fashion

Since loss of MSUT2 expression causes lengthening of poly(A) tails, we investigated whether generally reducing poly(A) tail lengths might affect tauopathy. The drug Cordycepin inhibits the addition of poly(A) to mRNAs (Rose et al., 1977; Wong et al., 2010). When we treated cultured human HEK293 cells that overexpress human tau with the compound cordycepin, we found a significant increase in phosphorylated tau (Fig. 1). This effect was blocked completely by co-treatment with RNAi against MSUT2 but not by PABPN1, confirming that MSUT2 specifically mediates the increase in pathological tau caused by inhibiting polyadenylation.

3.2. A reverse genetic survey of mRNA deadenylase function in a C. elegans model of tauopathy

We used our *C. elegans* model of tauopathy to examine whether loss of any of the poly(A) deadenylases might phenocopy the effects of loss of *sut-2* on tauopathy. Seven deadenylases have been identified in *C. elegans* via homology, belonging to the Ccr4-Not complex, the Pan2-Pan3 complex, or orthologs of individual deadenylase family members PARN, Angel, and 2′ phosphodiesterase (Nousch et al., 2013). In *C. elegans*, loss of the Ccr4-Not components caused significant lengthening of poly(A) tails, while loss of Pan2-Pan3 complex components or PARN genes did not cause longer poly(A) tails but only reduced the abundance of short poly(A) tails (Nousch et al., 2013). We obtained loss of function alleles (Table 1) that affected all known deadenylase complexes except for *pde-12*, whose homologs in other species are localized exclusively to mitochondria (Yan, 2014). We crossed them into our *C. elegans* tauopathy model and evaluated effects on tau-induced behavioral deficits (Fig. 2). We previously reported that loss of *ccr-4* enhanced tau-induced behavior deficits (Wheeler et al., 2019). Here we confirmed with a second allele that loss of *ccr-4* enhanced tau-induced behavior deficits. We also found that loss of *panl-2* enhanced tau-induced behavior deficits, loss of *parn-2* partially suppressed tau-induced behavior deficits, and *angl-1* and *panl-3* had no effect. Most of the alleles tested caused reduction in locomotor ability of ~10–20% in non-transgenic *C. elegans* (Supplemental Fig. 1), but the effects of each allele were significantly less on non-transgenic *C. elegans* than on tau transgenic *C. elegans*, suggesting that loss of these genes caused effects on tau-induced behavioral primarily through affecting tau toxicity. Although *angl-1* was evaluated due to its similarity to the mammalian Angel, it is unclear if this gene is important for poly(A) tail regulation in

C. elegans (Nousch et al., 2013). The fact that *panl-2* and *panl-3* did not have the same effect on tauopathy was surprising, since loss of either gene caused the same reduction in brood size of *C. elegans* raised at elevated temperatures (Nousch et al., 2013). Additionally, despite having different effects on tau, these deadenylases had similar effects on polyA tails in tau transgenic *C. elegans* (Supplemental Figure 2, Supplemental table 1). This suggests that the effects these deadenylases have on tauopathy may not correlate with their effects on other phenotypes.

3.3. The C. elegans PARN homolog parn-1 is epistatic to parn-2 with respect to tauopathy

Since we observed that only *parn-2* had significant effects on tau-induced behavioral deficits, we evaluated the effect of loss of both *parn-1* and *parn-2* on the same tau-induced behavioral deficits (Fig. 3). While loss of *parn-1* and *parn-2* had similar effects on poly(A) tail lengths in *C. elegans* (Nousch et al., 2013, Supplemental Figure 2), in human cell culture studies, the human homologs of *parn-1* and *parn-2*, PARN and TOE1 respectively, have shown sometimes overlapping and sometimes non-redundant effects on poly(A) tails of non-coding RNAs (Deng et al., 2019; Son et al., 2018). We found that loss of *parn-1* blocked the suppression of tauopathy caused by loss of *parn-2*. Interestingly this is opposite of the effect seen on brood size in *C. elegans*, where loss of *parn-2* blocked the fertility deficit caused by loss of *parn-1* in *C. elegans* raised at higher temperatures (Nousch et al., 2013). However, loss of *parn-2* does not block the lengthening of piwi-interacting RNAs (piRNA) induced by loss of *parn-1* (Tang et al., 2016). Our results suggest that in the modulation of tauopathy, *parn-1* is dominant over *parn-2*.

3.4. Loss of deadenylase function does not significantly alter tau aggregation

Next we evaluated whether loss of *ccr-4*, *panl-2*, *parn-1*, or *parn-2* had any effect on total tau protein levels or tau aggregation. We performed sequential extractions of tau protein and found no significant changes in total tau or insoluble tau levels by any of these genes (Fig. 4). This contrasts with *sut-2*, MSUT2, and PABPN1, which have been previously shown to alter levels of insoluble tau (Guthrie et al., 2009; Wheeler et al., 2019). However, the effects of these deadenylase genes on tauopathy behavior, which varied between a ~ 50% reduction and ~ 50% increase in locomotor ability, was less significant than loss of *sut-2* on tauopathy behavior which results in near complete rescue in locomotor ability (Guthrie et al., 2009); it is therefore possible that a significant change in tau protein aggregation was not detectable. Alternatively, the modulation of tau-induced behavioral phenotypes by these deadenylase genes may occur independent of modulating tau protein levels.

3.5. SUT-2 modulation of tauopathy is epistatic to parn-2 and ccr-4

Although the various deadenylases we examined did not have the same effects on tauopathy as *sut-2*, since they all can interact with poly (A), they might affect how *sut-2* modulates tauopathy. We investigated whether loss of *parn-2*, which suppresses tauopathy, could block enhancement caused by overexpression of SUT-2 and whether loss of *ccr-4*, which enhances tauopathy, could block suppression caused by loss of *sut-2*. We found that loss of *parn-2* did not rescue the enhancement of tauopathy caused by overexpression of SUT-2 protein (Fig. 5a). We also found that loss of *ccr-4* did not block suppression of tauopathy by loss of *sut-2*

(Fig. 5b). This shows that *sut-2* is epistatic to both *parn-2* and *ccr-4* in regulation of tauopathy.

3.6. MSUT2 does not colocalize with poly(A) deadenylases

Because *sut-2* was epistatic to *parn-2* and *ccr-4* in regulating tauopathy, we investigated whether this could be due to close interactions between *sut-2*/MSUT2 and poly(A) deadenylases in our tauopathy model. In cells, SUT-2/MSUT2 localizes to nuclear speckles (Guthrie et al., 2009; Wheeler et al., 2019), while various poly(A) deadenylases are found in the nucleus or cytoplasm, in Cajal bodies and/or P bodies (Yan, 2014). However, the localization of these deadenylases could be altered in tauopathy. Using cultured human HEK293 cells overexpressing human tau protein, we coimmunostained for MSUT2 and the human homologs of *ccr-4* (CNOT6), *panl-2* (PAN2), *parn-1* (PARN), and *parn-2* (TOE1) (Fig 6). Staining for CNOT6, PAN2, PARN, and TOE1 was similar to what was reported in previous literature (Bett et al., 2013; Deng et al., 2019; Mittal et al., 2011; Son et al., 2018). We found little co-localization of immunostaining between MSUT2 and any of these deadenylases. While immunostaining studies do not exclude the possibility of transient or limited interactions between MSUT2 and these deadenylases, it does suggest that the majority of MSUT2 protein exists in separate cellular compartmentsrelative to the deadenylases. This suggests that SUT-2/MSUT2 may not be blocking the effects of deadenylases on tauopathy via direct interactions.

3.7. TOE1 expression correlates with MSUT2 expression in Alzheimer's disease brains

Since loss of *parn-2/TOE1* suppresses tau toxicity in our *C. elegans* model but its effect is blocked by overexpression of SUT-2, we investigated whether expression of TOE1 correlated with MSUT2 expression in Alzheimer's disease. We previously demonstrated MSUT2 depletion correlates with disease severity in AD patients (increase in phosphorylated tau and increased neuronal loss) (Wheeler et al., 2019). In the current study, we found that neurons in the frontal cortex of postmortem brain tissue from these same AD brain donors with depleted MSUT2 also exhibited reduced TOE1 immunoreactivity. In contrast, AD donor brains with normal levels of MSUT2 demonstrated robust levels of TOE1, comparable to TOE1 immunoreactivity in normal control cases (Table 2, Fig. 7a,b). This TOE1 staining was primarily cytoplasmic in both normal and Alzheimer's disease patient brains with no gross differences in intensity (Fig. 7b). Thus, compared to cases with normal levels of TOE1, cases with reduced TOE1 expression exhibited greater accumulation of pathological tau (Fig 7c,d) and increased loss of NeuN positive neurons (Fig. 7e,f). Taken together these data suggest that the mechanisms altering MSUT2 expression in Alzheimer's disease also affect TOE1 expression.

4. Discussion

Cordycepin has been previously demonstrated to limit polyadenylation by acting as a poly(A) polymerase inhibitor (Rose et al., 1977; Wong et al., 2010). Although inhibiting polyadenylation with the chemical inhibitor cordycepin exacerbated pathological tau accumulation, if poly(A) tail length regulation was the only mechanism by which *sut-2* modulated tauopathy, then loss of poly(A) deadenylase activity, which increases poly(A) tail

length, would all have the same effect on tauopathy as *sut-2*. By screening various poly(A) deadenylases for modulation of pathological tau, we have found both deadenylases that enhance tau toxicity when lost (*ccr-4*, *panl-2*) and suppress tau toxicity when lost (*parn-2*) even though they had similar effects on poly(A) tail length. Thus poly(A) tail length regulation alone fails to explain the impact of any deadenylases on tauopathy. Furthermore, despite different mechanisms and cellular localizations, *sut-2* was epistatic to *ccr-4* and *parn-2* in modulating tauopathy. Our data suggest that poly(A) deadenylases and *sut-2* regulate tauopathy indirectly through poorly understood non-poly(A) mediated mechanisms.

It is unclear how deadenylases modulate behavioral deficits caused by tau overexpression in tau transgenic *C. elegans* when they cause no detectable change in tau protein levels or solubility. One possibility is that there is still a change in the conformation of tau protein that affects its toxicity despite no change in solubility. Another possibility is that toxic tau interacts with substrates that are upregulated when deadenylase activity is lost, causing a change in toxicity. For example, perhaps loss of deadenylases changes the availability of tau binding partners permitting additional tau-tau self-association and initiation of a toxic aggregation cascade.

Interestingly, even though *parn-2/TOE1* differs from *sut-2/MSUT2* in terms of function and cellular localization, TOE1 and MSUT2 expression varied in the same way in Alzheimer's disease brains. This suggests a similar mechanism may lead to TOE1 and MSUT2 downregulation in earlier onset Alzheimer's disease. However, whether TOE1 and MSUT2 expression becomes downregulated simultaneously, sequentially, or independently is impossible to discern from study of postmortem human tissue.

It is unclear mechanistically how *TOE1* works in aging and neurodegenerative diseases of aging. Familial loss of function mutations in *TOE1* have been shown to cause pontocerebellar hypoplasia type 7, where neurodegeneration in patient brains occurs so early it overlaps with neurodevelopment (Lardelli et al., 2017). Otherwise in mitotic cells, TOE1 has been shown to modulate small nuclear RNA and telomerase RNA maturation (Deng et al., 2019; Son et al., 2018). The fact that PARN has a similar function in regulating non-coding RNA (ncRNA) and telomerase RNA function but acts as a mild enhancer of tau toxicity instead indicates that general defects in ncRNA and telomerase RNA function do not explain suppression of tau toxicity by *parn-2* in tau transgenic *C. elegans*. However, *TOE1* knockdown in HeLa cells affected some ncRNA that *PARN* knockdown did not (Deng et al., 2019; Son et al., 2018), so perhaps the regulation of specific targets leads to suppression versus enhancement of tau toxicity. Additionally, while specific regulation of piRNA length has been ascribed to *parn-1* in *C. elegans* (Tang et al., 2016), no unique roles have been identified yet for *parn-2*. Further investigation into the distinct functions of *parn-1* and *parn-2* as well as better understanding of the role of *parn-2/TOE1* in post-mitotic cells like adult neurons may shed more light on its ability to modulate tauopathy and bring a more precise mechanistic understanding of why *parn-2/TOE1* has an effect on tauopathy while the related deadenylase *parn-1/PARN* did not, and why it has opposite effects on tauopathy compared to other deadenylases *panl-2* and *ccr-4*.

With triple mutant analysis we observed that *sut-2* is epistatic to *parn-2* and *ccr-4*. This suggests that *sut-2* may interact downstream of *parn-2* and *ccr-4* pathways in modulating tau toxicity. Perhaps this is through reversing the effects of *parn-2* and *ccr-4* on tau-induced toxicity. Another possibility is that instead of acting downstream of *parn-2* and *ccr-4* in modulating tau toxicity, *sut-2* interacts with tau upstream of the pathways that allow *parn-2* and/or *ccr-4*-related pathways to interact with tau, diverting tau away from interactions with *parn-2* or *ccr-4*.

Evidence that could support the latter idea is as follows. Previous work has suggested a variety of polyanions as a disease relevant molecular driver of aggregation seeding necessary to overcome charge repulsion between tau monomers (Friedhoff et al., 1998; Kuret et al., 2005). Indeed, recent work on tau fibril structure has shown that an uncharacterized polyanion resides in the core of corticobasal degeneration tau fibrils (Zhang et al., 2020). More specifically, in vitro tau forms complexes with RNA that potently seed tau fibril formation (Kampers et al., 1996). Furthermore, tau's interaction with and polymerization of microtubules is disrupted by poly(A) RNA (Bryan et al., 1975; Kampers et al., 1996). Thus, one hypothesis is that MSUT2 is changing the availability of free RNA available to tau in the cytoplasm. Under this scenario, loss of *sut-2/MSUT2* could reduce interactions between cellular poly(A) RNA and tau while overexpression of SUT-2/MSUT2 could promote interactions between RNA and tau that preclude interference by poly(A) polymerases. Therefore, the work described here can be viewed as a first probing of the in vivo mechanisms of RNA triggered tau aggregation.

In summary, we found that modulation of tauopathy by various poly (A)-related genes is not as simple as regulating bulk polyadenylation state. We found multiple deadenylases can modulate tauopathy, meriting further investigation into poly(A) regulating genes and tauopathy. We also identified a new link between *parn-2/TOE1* and tauopathy with evidence that TOE1 expression correlates with disease severity in Alzheimer's patients. Additional work is now necessary to determine how *parn-2/TOE1* and *sut-2/MSUT2* modulates disease mechanisms in tauopathy and how the many cellular deadenylases might differentially impact accumulation of pathological tau This includes investigating *parn-2/TOE1* and *sut-2/MSUT2* functions and molecular binding partners. While MSUT2 may be a promising target for tauopathy treatments (Wheeler et al., 2019), this study suggests expanding the scope of tau related therapeutic targets into other RNA metabolism regulating genes may be fruitful.

Supplementary Material

Refer to Web version on PubMed Central for supplementary material.

Acknowledgements

We thank Kaili Chickering, Jeanna Wheeler, Aristide Black, and Elaine Loomis for outstanding research assistance. We thank Erica Melief for outstanding administrative assistance. We thank the National Bioresource Project (Japan) and *C. elegans* Genetics Center (CGC) for providing strains. We thank WormBase for essential *C. elegans* model organism information. We thank the Developmental Studies Hybridoma Bank (NICHD) for the β-tubulin primary antibody E7. We thank Peter Davies and Virginia Lee for anti-tau antibodies. We thank the Developmental Studies Hybridoma Bank (NICHD) for the β-tubulin antibody E7.

Funding

This work was supported by grants from the Department of Veterans Affairs [Merit Review Grant #I01BX002619 to B·K., Career Development Award 2 #IK2BX007080 to RK]; National Institutes of Health (# RF1AG055474 and # R01NS064131 to B.K, K08 AG065426 to C.L., P50AG005136 and U01AG006781 to C.D.K. for the UW ADRC and Adult Changes in Thought study) as well as the Nancy and Buster Alvord endowment (C.D.K).

References

Arribere JA, Bell RT, Fu BXH, Artiles KL, Hartman PS, Fire AZ, 2014. Efficient marker-free recovery of custom genetic modifications with CRISPR/Cas9 in caenorhabditis elegans. Genetics 198, 837–846. 10.1534/genetics.114.169730. [PubMed: 25161212]

Bett JS, Ibrahim AFM, Garg AK, Kelly V, Pedrioli P, Rocha S, Hay RT, 2013. The P-body component USP52/PAN2 is a novel regulator of HIF1A mRNA stability. Biochem. J 451, 185–194. 10.1042/BJ20130026. [PubMed: 23398456]

Bierer LM, Hof PR, Purohit DP, Carlin L, Schmeidler J, Davis KL, Perl DP, 1995. Neocortical neurofibrillary tangles correlate with dementia severity in Alzheimer's disease. Arch. Neurol 52, 81–88. 10.1001/archneur.1995.00540250089017. [PubMed: 7826280]

Brenner S, 1974. The genetics of Caenorhabditis elegans. Genetics 77, 71–94. [PubMed: 4366476]

Bryan J, Nagle BW, Doenges KH, 1975. Inhibition of tubulin assembly by RNA and other polyanions: evidence for a required protein. Proc. Natl. Acad. Sci. U. S. A 72, 3570–3574. [PubMed: 1059144]

Deng T, Huang Y, Weng K, Lin S, Li Y, Shi G, Chen Y, Huang J, Liu D, Ma W, Songyang Z, 2019. TOE1 acts as a 3′ exonuclease for telomerase RNA and regulates telomere maintenance. Nucleic Acids Res. 47, 391–405. 10.1093/nar/gky1019. [PubMed: 30371886]

Eckmann CR, Rammelt C, Wahle E, 2011. Control of poly(A) tail length. Wiley Interdiscip. Rev. RNA 2, 348–361. 10.1002/wrna.56. [PubMed: 21957022]

Friedhoff P, Von Bergen M, Mandelkow EM, Davies P, Mandelkow E, 1998. A nucleated assembly mechanism of Alzheimer paired helical filaments. Proc. Natl. Acad. Sci. U. S. A 95, 15712–15717. 10.1073/pnas.95.26.15712. [PubMed: 9861035]

Gaugler J, James B, Johnson T, Scholz K, Weuve J, 2016. 2016 Alzheimer's disease facts and figures. Alzheimers Dement. 12, 459–509. 10.1016/j.jalz.2016.03.001. [PubMed: 27570871]

Guthrie CR, Schellenberg GD, Kraemer BC, 2009. SUT-2 potentiates tau-induced neurotoxicity in Caenorhabditis elegans. Hum. Mol. Genet 18, 1825–1838. 10.1093/hmg/ddp099. [PubMed: 19273536]

Irwin DJ, 2016. Tauopathies as clinicopathological entities. Parkinsonism Relat. Disord 22, S29–S33. 10.1016/j.parkreldis.2015.09.020. [PubMed: 26382841]

Kampers T, Friedhoff P, Biernat J, Mandelkow EM, Mandelkow E, 1996. RNA stimulates aggregation of microtubule-associated protein tau into Alzheimer-like paired helical filaments. FEBS Lett. 399, 344–349. 10.1016/S0014-5793(96)01386-5. [PubMed: 8985176]

Kelly SM, Leung SW, Pak C, Banerjee A, Moberg KH, Corbett AH, 2014. A conserved role for the zinc finger polyadenosine RNA binding protein, ZC3H14, in control of poly(A) tail length. Rna 20, 681–688. 10.1261/rna.043984.113. [PubMed: 24671764]

Khanna MR, Kovalevich J, Lee VMY, Trojanowski JQ, Brunden KR, 2016. Therapeutic strategies for the treatment of tauopathies: hopes and challenges. Alzheimers Dement. 12, 1051–1065. 10.1016/j.jalz.2016.06.006. [PubMed: 27751442]

Kow RL, Sikkema C, Wheeler JM, Wilkinson CW, Kraemer BC, 2018. DOPA decarboxylase modulates tau toxicity. Biol. Psychiatry 83, 438–446. 10.1016/j.biopsych.2017.06.007. [PubMed: 28751068]

Kraemer BC, Schellenberg GD, 2007. SUT-1 enables tau-induced neurotoxicity in C. elegans. Hum. Mol. Genet 16, 1959–1971. 10.1093/hmg/ddm143. [PubMed: 17576746]

Kraemer BC, Zhang B, Leverenz JB, Thomas JH, Trojanowski JQ, Schellenberg GD, 2003. Neurodegeneration and defective neurotransmission in a Caenorhabditis elegans model of tauopathy. Proc. Natl. Acad. Sci. U. S. A 100, 9980–9985. 10.1073/pnas.1533448100. [PubMed: 12872001]

Kraemer BC, Burgess JK, Chen JH, Thomas JH, Schellenberg GD, 2006. Molecular pathways that influence human tau-induced pathology in Caenorhabditis elegans. Hum. Mol. Genet 15, 1483–1496. 10.1093/hmg/ddl067. [PubMed: 16600994]

Kuret J, Chirita CN, Congdon EE, Kannanayakal T, Li G, Necula M, Yin H, Zhong Q, 2005. Pathways of tau fibrillization. Biochim. Biophys. Acta Mol. basis Dis 1739, 167–178. 10.1016/j.bbadis.2004.06.016.

Lardelli RM, Schaffer AE, Eggens VRC, Zaki MS, Grainger S, Sathe S, Van Nostrand EL, Schlachetzki Z, Rosti B, Akizu N, Scott E, Silhavy JL, Heckman LD, Rosti RO, Dikoglu E, Gregor A, Guemez-Gamboa A, Musaev D, Mande R, Widjaja A, Shaw TL, Markmiller S, Marin-Valencia I, Davies JH, De Meirleir L, Kayserili H, Altunoglu U, Freckmann ML, Warwick L, Chitayat D, Blaser S, Ça Layan AO, Bilguvar K, Per H, Fagerberg C, Christesen HT, Kibaek M, Aldinger KA, Manchester D, Matsumoto N, Muramatsu K, Saitsu H, Shiina M, Ogata K, Foulds N, Dobyns WB, Chi NC, Traver D, Spaccini L, Bova SM, Gabriel SB, Gunel M, Valente EM, Nassogne MC, Bennett EJ, Yeo GW, Baas F, Lykke-Andersen J, Gleeson JG, 2017. Biallelic mutations in the 3′ exonuclease TOE1 cause pontocerebellar hypoplasia and uncover a role in snRNA processing. Nat. Genet 49, 457–464. 10.1038/ng.3762. [PubMed: 28092684]

Lima SA, Chipman LB, Nicholson AL, Chen YH, Yee BA, Yeo GW, Coller J, Pasquinelli AE, 2017. Short poly(A) tails are a conserved feature of highly expressed genes. Nat. Struct. Mol. Biol 24, 1057–1063. 10.1038/nsmb.3499. [PubMed: 29106412]

McCormick AV, Wheeler JM, Guthrie CR, Liachko NF, Kraemer BC, 2013. Dopamine D2 receptor antagonism suppresses tau aggregation and neurotoxicity. Biol. Psychiatry 73, 464–471. 10.1016/j.biopsych.2012.08.027. [PubMed: 23140663]

Mittal S, Aslam A, Doidge R, Medica R, Winkler GS, 2011. The Ccr4a (CNOT6) and Ccr4b (CNOT6L) deadenylase subunits of the human Ccr4-not complex contribute to the prevention of cell death and senescence. Mol. Biol. Cell 22, 748–758. 10.1091/mbc.E10-11-0898. [PubMed: 21233283]

Nousch M, Techritz N, Hampel D, Millonigg S, Eckmann CR, 2013. The Ccr4-not deadenylase complex constitutes the main poly(A) removal activity in C. elegans. J. Cell Sci 126, 4274–4285. 10.1242/jcs.132936. [PubMed: 23843623]

Paix A, Folkmann A, Rasoloson D, Seydoux G, 2015. High efficiency, homology-directed genome editing in Caenorhabditis elegans using CRISPR-Cas9ribonucleoprotein complexes. Genetics 201, 47–54. 10.1534/genetics.115.179382. [PubMed: 26187122]

Riley KP, Snowdon DA, Markesbery WR, 2002. Alzheimer's neurofibrillary pathology and the spectrum of cognitive function: findings from the Nun study. Ann. Neurol 51, 567–577. 10.1002/ana.10161. [PubMed: 12112102]

Rose KM, Bell LE, Jacob ST, 1977. Selective inhibition of initial polyadenylation in isolated nuclei by low levels of cordycepin 5′-triphosphate. BBA Sect. Nucleic Acids Protein Synth 475, 548–552. 10.1016/0005-2787(77)90069-7.

Son A, Park JE, Kim VN, 2018. PARN and TOE1 constitute a 3′ end maturation module for nuclear non-coding RNAs. Cell Rep. 23, 888–898. 10.1016/j.celrep.2018.03.089. [PubMed: 29669292]

Tang W, Tu S, Lee HC, Weng Z, Mello CC, 2016. The RNase PARN-1 trims piRNA 3′ ends to promote transcriptome surveillance in C. elegans. Cell 164, 974–984. 10.1016/j.cell.2016.02.008. [PubMed: 26919432]

Tiraboschi P, Hansen LA, Thal LJ, Corey-Bloom J, 2004. The importance of neuritic plaques and tangles to the development and evolution of AD. Neurology 62, 1984–1989. 10.1212/01.WNL.0000129697.01779.0A. [PubMed: 15184601]

Wang Y, Mandelkow E, 2016. Tau in physiology and pathology. Nat. Rev. Neurosci 17, 5–21. 10.1038/nrn.2015.1. [PubMed: 26631930]

Wheeler JM, McMillan P, Strovas TJ, Liachko NF, Amlie-Wolf A, Kow RL, Klein RL, Szot P, Robinson L, Guthrie C, Saxton A, Kanaan NM, Raskind M, Peskind E, Trojanowski JQ, Lee VMY, Wang L-S, Keene CD, Bird T, Schellenberg GD, Kraemer B, 2019. Activity of the poly(A) binding protein MSUT2 determines susceptibility to pathological tau in the mammalian brain. Sci. Transl. Med 11 10.1126/scitranslmed.aao6545 eaao6545.

Wong YY, Moon A, Duffin R, Barthet-Barateig A, Meijer HA, Clemens MJ, De Moor CH, 2010. Cordycepin inhibits protein synthesis and cell adhesion through effects on signal transduction. J. Biol. Chem 285, 2610–2621. 10.1074/jbc.M109.071159. [PubMed: 19940154]

Yan Y. Bin, 2014. Deadenylation: enzymes, regulation, and functional implications. Wiley Interdiscip. Rev. RNA 5, 421–443. 10.1002/wrna.1221. [PubMed: 24523229]

Zhang X, Virtanen A, Kleiman FE, 2010. To polyadenylate or to deadenylate: that is the question. Cell Cycle 9, 4437–4449. 10.4161/cc.9.22.13887. [PubMed: 21084869]

Zhang W, Tarutani A, Newell KL, Murzin AG, Matsubara T, Falcon B, Vidal R, Garringer HJ, Shi Y, Ikeuchi T, Murayama S, Ghetti B, Hasegawa M, Goedert M, Scheres SHW, 2020. Novel tau filament fold in corticobasal degeneration. Nature 580. 10.1038/s41586-020-2043-0.

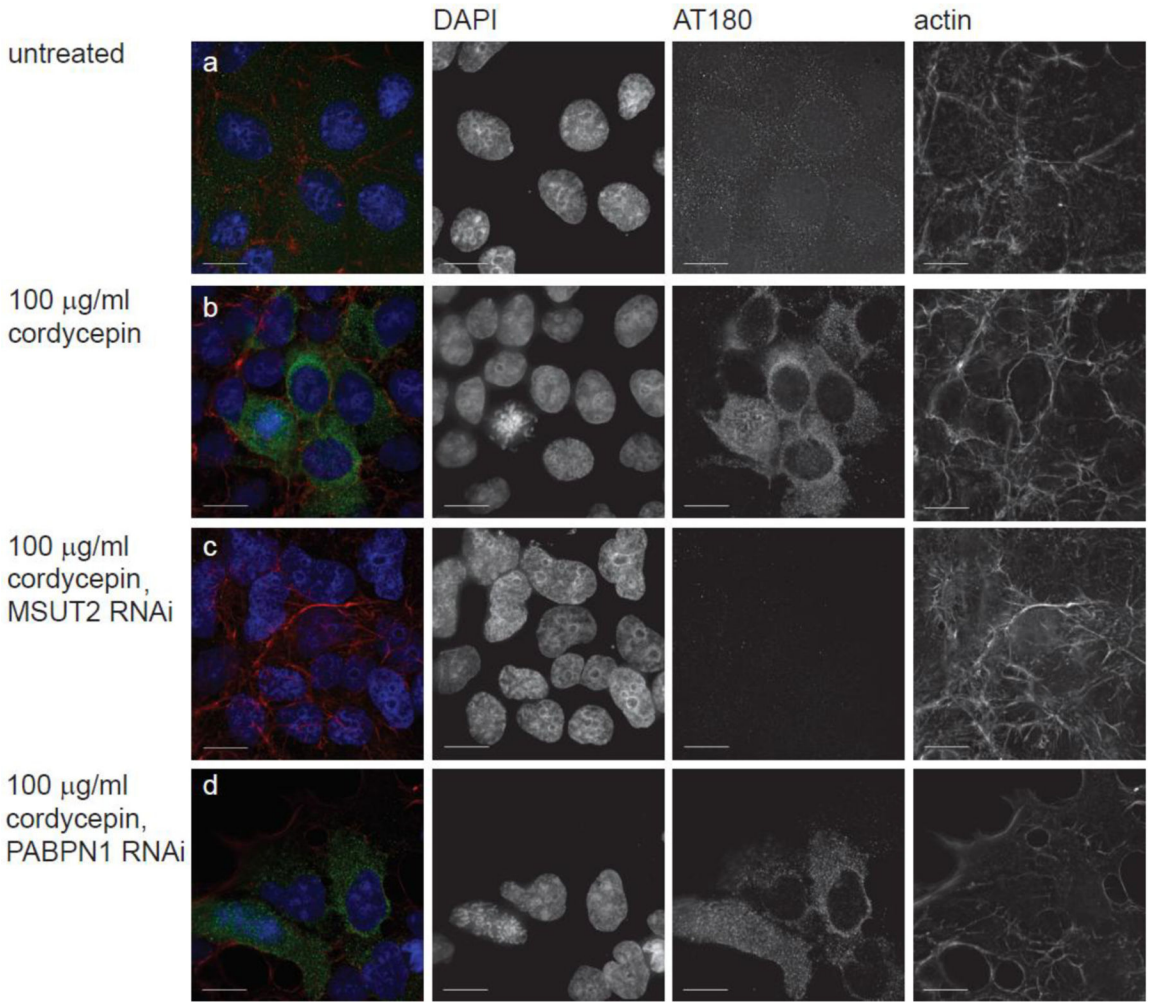

Fig. 1.

General inhibition of Poly(A) addition by cordycepin increases pathological tau in a MSUT2-dependent manner. Immunocytochemistry staining of HEK293 cells overexpressing tau protein with DAPI (blue), AT180 (detects phospho Thr231 of tau protein) (green), and actin (red). (a) HEK293 cells overexpressing human tau protein. (b) HEK293 cells overexpressing human tau protein treated with 100 μg/mL cordycepin. (c) HEK293 cells overexpressing human tau protein treated with 100 μg/mL cordycepin and MSUT2 RNAi. (d) HEK293 cells overexpressing human tau protein treated with 100 μg/mL cordycepin and PABPN1 RNAi. The RNAi knockdown efficiency for MSUT2 and PABPN1 was similar to that published previously (Wheeler et al., 2019). Scale bars = 15 μm.

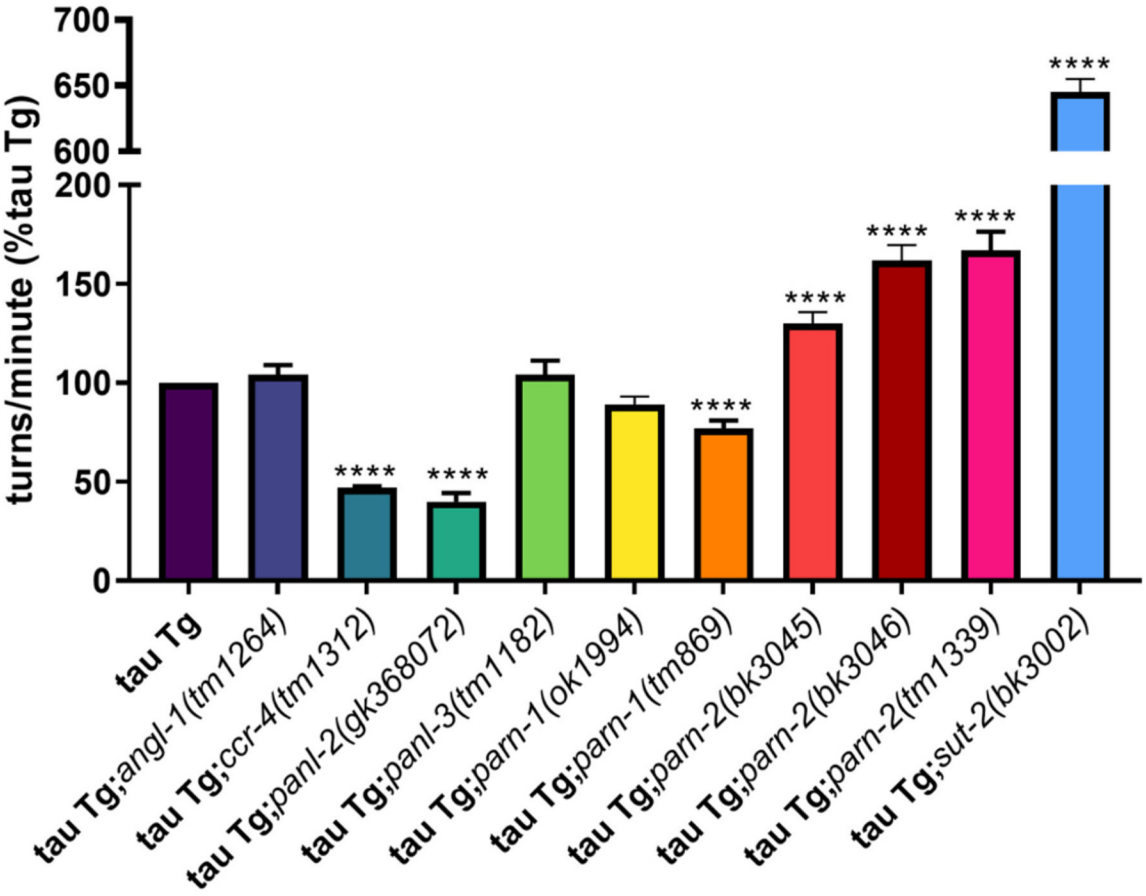

Fig. 2.

Loss of function in various poly(A) deadenylase genes have varied effects on tau-induced behavior deficits in tau transgenic *C. elegans*. Swimming assays in M9 buffer were performed on 4-day-old tau transgenic (tau Tg) *C. elegans* (roughly day 1 adulthood). At least 100 worms per strain were analyzed by video software and frequency of body bends (turns) were calculated and normalized to control (tau Tg) for each double mutant. Error bars are means ± SEM. Student's *t*-tests were used to determine significance of double mutant versus tau Tg. **** $p < < 0.0001$ when compared to tau Tg.

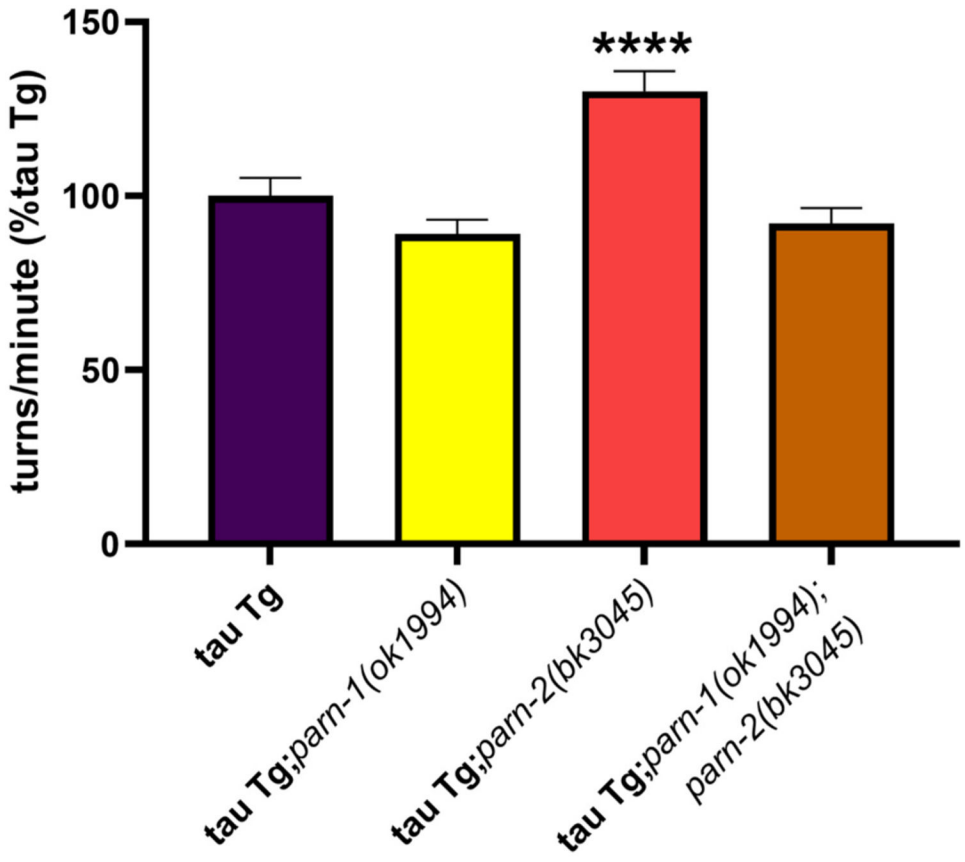

Fig. 3.

Loss of *parn-1* blocks the suppression of tau-induced behavioral deficits seen with loss of *parn-2*. Swimming assays in M9 buffer were performed on 4-day-old tau transgenic (tau Tg) *C. elegans* (roughly day 1 adulthood). At least 100 worms per strain were analyzed by video software and frequency of body bends (turns) was calculated. Error bars are means ± SEM. **** $p << 0.0001$ when compared to tau Tg. Statistical significance was determined by two-way ANOVA followed by Tukey's multiple comparisons tests. There was no significant difference between tau Tg;*parn-1* and tau Tg;*parn-1;parn-2* worms.

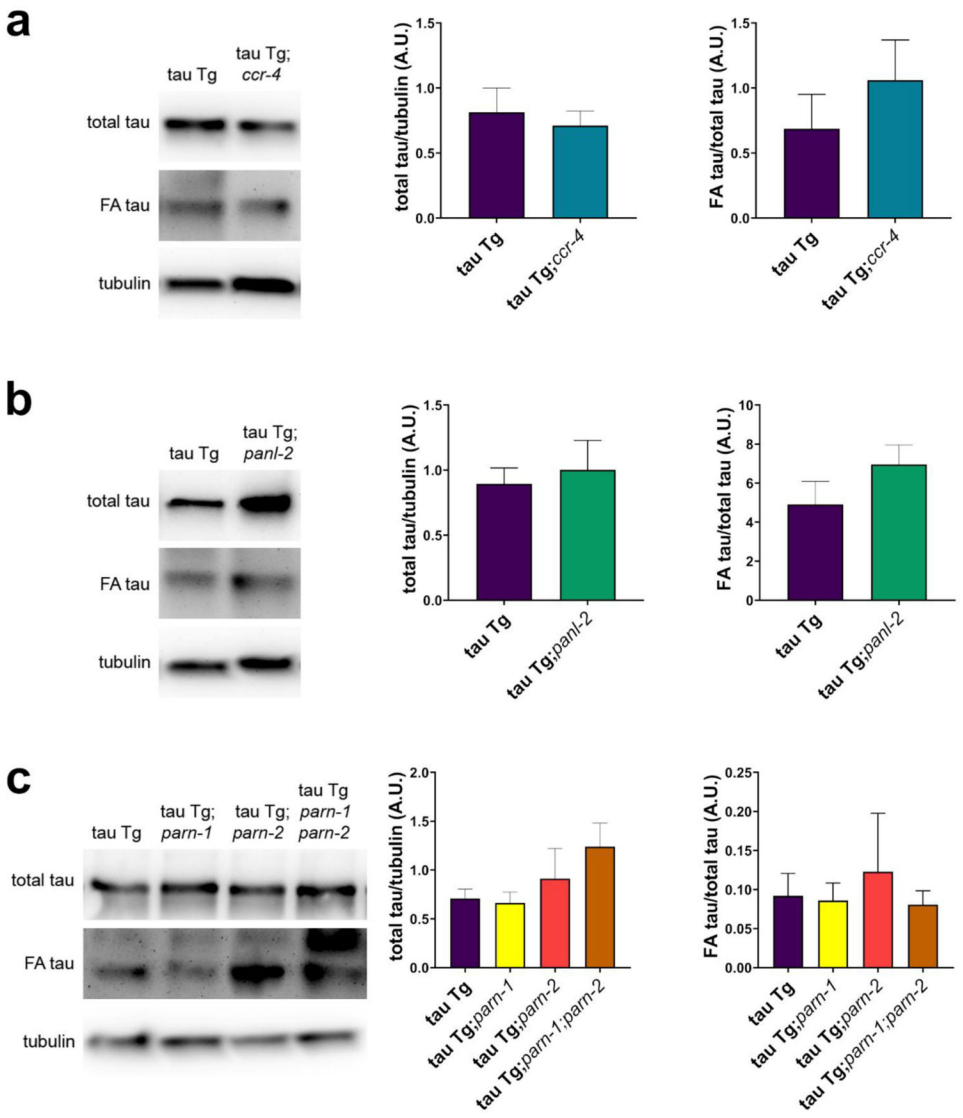

Fig. 4.

Loss of deadenylase genes did not significantly alter levels of total tau or insoluble tau protein. Lysates of 3-day-old tau transgenic *C. elegans* and double mutants were subjected to sequential extraction and total tau, insoluble formic-acid (FA) tau, and tubulin were detected by immunoblot. (a) Comparison of tau protein levels in tau Tg and tau Tg;*ccr-4*. (b) Comparison of tau protein levels in tau Tg and tau Tg;*panl-2*. (c) Comparison of tau protein levels in tau Tg and tau Tg;*parn-1*, tau Tg;*parn-2*, and tau Tg;*parn-1;parn-2*. Error bars are means — SEM. At least 3 replicates were analyzed per comparison. Student's *t*-test was used for tau Tg vs tau Tg;*ccr-4* or tau Tg;*panl-2* comparisons, while one-way ANOVA for tau Tg vs tau Tg;*parn-1*, tau Tg;*parn-2*, and tau Tg;*parn-1;parn-2* to determine statistical significance. No comparisons were significant.

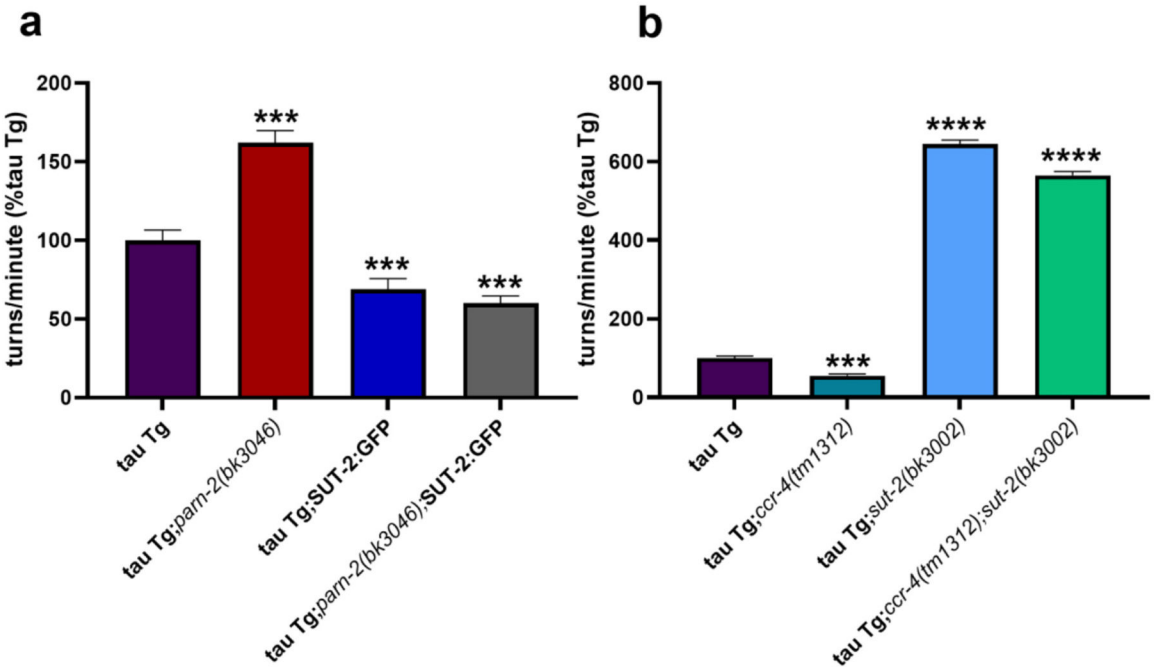

Fig. 5.

Loss of *parn-2* and *ccr-4* do not modulate effects of SUT-2 overexpression and *sut-2* deletion respectively in tau transgenic *C. elegans*. Swimming assays in M9 buffer were performed on 4-day-old tau transgenic (tau Tg) *C. elegans* (roughly day 1 adulthood). At least 100 worms per strain were analyzed by video software and frequency of body bends (turns) were calculated. Error bars are means ± SEM. *** $p < 0.005$ **** $P < < 0.0001$ when compared to tau Tg. (a) Comparison of tau Tg *C. elegans* to tau Tg;*parn-2*, tau Tg;SUT-2:GFP, and tau Tg;*parn-2*;SUT-2:GFP worms. There was no significant difference between tau Tg;SUT-2:GFP and tau Tg;*parn-2*; SUT-2:GFP worms. (b) Comparison of tau Tg *C. elegans* to tau Tg;*ccr-4*, tau Tg;*sut-2*, and tau Tg;*ccr-4;sut-2* worms. Statistical significance was determined by two-way ANOVA followed by Tukey's multiple comparisons tests.

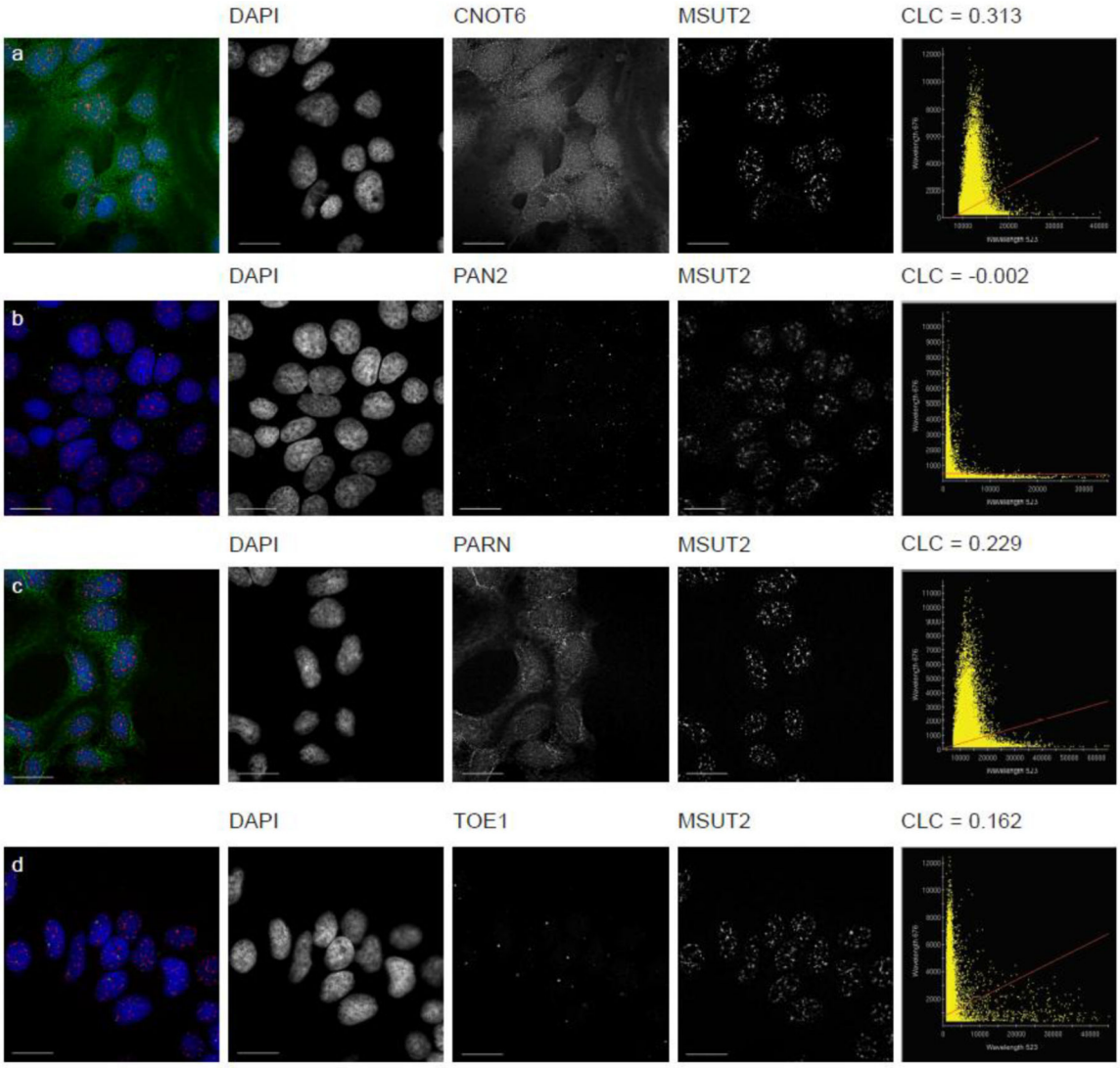

Fig. 6.

Poly(A) deadenylases do not colocalize with MSUT2. Immunocytochemistry of HEK293 cells overexpressing human tau protein with DAPI (blue), MSUT2 (red), and deadenylase of interest (green). Colocalization (CLC) plots indicate amount of signal overlap between MSUT2 and deadenylase of interest. (a) Comparison of CNOT6 and MSUT2. (b) Comparison of PAN2 and MSUT2. (c) Comparison of PARN and MSUT2. (d) Comparison of TOE1 and MSUT2. Scale bars = 15 μm.

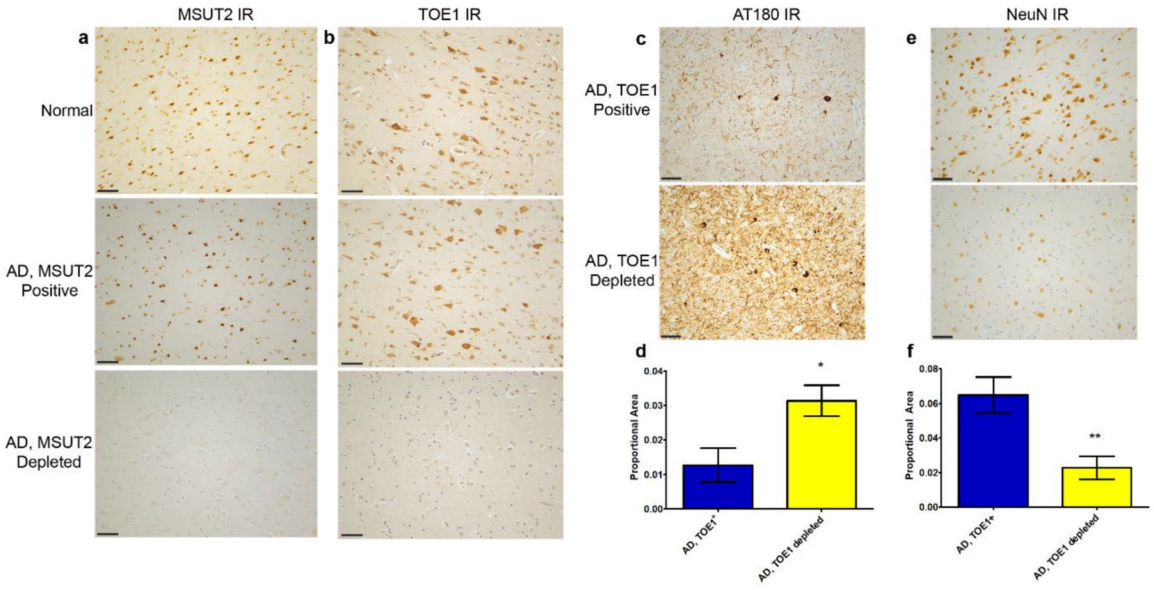

Fig. 7.

TOE1 expression levels parallel MSUT2 expression levels in Alzheimer's disease brain, suggesting the mechanisms altering MSUT2 expression and tauopathy may also affect TOE1 expression. Representative brain sections of postmortem brain frontal cortex from a neurologically normal control and an MSUT2 positive or MSUT2 depleted AD case stained with MSUT2 (a) or TOE1 (b). AD cases that were positive for MSUT2 had robust levels of TOE1, while AD cases depleted of MSUT2 were also deficient in TOE1 immunoreactivity. Representative sections of postmortem cerebral cortex from TOE1 positive or TOE1 depleted AD cases stained with AT180 (detects phospho Thr231 of tau protein) (c) or NeuN (e). The AD brains with depleted levels of mSUT2 (a) and TOE1 (b) demonstrated increased pTau burden (c,d) and increased neuronal loss as indicated by a decrease in NeuN immunoreactivity (e,f). (d,f) Densitometry analysis of AT180 and NeuN positive reactivity in TOE1 positive AD cases ($n = 8$) compared to TOE1 depleted AD cases ($n = 7$). (AT180, $*p = 0.015$ and NeuN, $**p = 0.0056$ by two-tailed Student's t-test). Scale bars = 100 μm.

Table 1

List of *C. elegans* genes of interest and alleles tested.

***C. elegans* gene**	**Closest human homolog**	**Alleles tested**	**Molecular change**
angl-1	ANGEL	*tm1264*	Deletion
ccr-4	CNOT6	*tm1312*	Deletion
panl-2	PAN 2	*gk368072*	Q474Ochre
panl-3	PAN 3	*tm1182*	Deletion
parn-1	PARN	*ok1994*	Deletion
		tm869	Deletion
parn-2	TOE1	*tm1339*	Deletion
		bk3045	Deletion
		bk3046	Deletion
sut-2	MSUT2	*bk3002*	Deletion

Table 2

Characteristics of human AD cases.

Case ID	NPDX	AGE	SEX	ONS	DU	PMI	CERAD	Braak	MSUT2	TOE1
UWA730	AD	100	**F**	82	18	3:08	Moderate	VI	High	High
UWA763	AD	91	**M**	82	9	7:00	Moderate	VI	High	High
UWA771	AD	86	**M**	81	5	4:25	Frequent	VI	High	High
UWA1501	AD	77	**M**	71	6	6:32	Frequent	VI	High	High
UWA1518	AD	77	**M**	63	14	5:20	Frequent	IV	High	High
UWA1550	AD	94	**M**	82	12	4:25	Frequent	VI	High	High
UWA2385	AD	86	**F**	76	10	8:32	Frequent	VI	High	High
UWA3556	AD	89	**M**	86	3	6:25	Frequent	V	High	High
UWA797	AD	62	**M**	55	7	4:32	Frequent	VI	High	Low
UWA732	AD	89	**F**	82	7	5:23	Moderate	V	Low	Low
UWA1443	AD	84	**F**	76	8	4:47	Frequent	V	Low	Low
UWA3554	AD	77	**M**	57	20	7:25	Frequent	VI	Low	Low
UWA6511	AD	90	**F**	76	14	6:23	Frequent	VI	Low	Low
UWA6542	AD	70	**F**	62	8	5:00	Frequent	VI	Low	Low
UWA6589	AD	68	**M**	58	10	9:25	Frequent	VI	Low	Low

NPDX = neuropathology diagnosis.

ONS = onset.

DU = duration (years).

PMI = post-mortem interval (hours:minutes).